The solar oblateness and its relationship with the structure of the tachocline and of the Sun's subsurface

S. Godier and J.-P. Rozelot

Observatoire de la Côte d'Azur, Département CERGA UMR 6527 du C.N.R.S., avenue Copernic,
06130 Grasse, France (godier; rozelot@obs-azur.fr)

Abstract. The solar oblateness ε was computed with a dynamical up-to-date solar model of mass and density, combined with a recent rotational model established from the helioseismic data, and including the effects of differential rotation with depth. To determine the theoretical value of the oblateness ε of the Sun, we integrated the extended differential equation governing the fluids in hydrostatic equilibrium and the Poisson equation for the gravitational potential. From this analysis, we deduced the profiles of ε, as a function of the radius and of the latitude, from the core to the surface, for a Sun splitted into a series of concentric shells. As each shell is affected by a potential distortion, mainly due to the rotation, and as the rotation rate depends on the radius and on the latitude, each shell of the Sun is affected by a different oblateness.

As a result of the integration of this function, we found $\varepsilon = 8.77.10^{-6}$, that we compared to the oblateness of a rigidly rotating sphere.

To interpret the difference in oblateness ε of the studied layers within the Sun, we linked the profiles to the solar interior structures, specially to the tachocline and to the subsurface, that help us to understand why and how these regions are mainly governed by shear. In particular, we propose for these two layers a double structure, one where the magnetic field would be stored and one of shear.

Finally, we compared our results of radial integrated oblateness with the latitudinal variation of the semidiameter from solar astrolabe observations.

Key words: Sun: fundamental parameters – Sun: interior – Sun: rotation – Sun: transition region

1. Introduction

Solar oblateness is a fundamental property of the Sun and its value is a direct input for some astrophysical computations. This is mainly the case for precise determination of planetary orbits and specially for the motion of Mercury and other minor planets, such as Icarus. The solar oblateness, if one is able to measure its value with a high accuracy, could be used to determine the Eddington-Robertson parameter (β) in the Parametrized-Post-Newtonian theories of gravity. This oblateness, which is linked to the internal structure, via its gravitational and rotational potentials, permits one to access certain physical properties of the layers below the surface. This is certainly the most interesting feature which has not yet been too much approached. Such features may concern at first the borderlines of the different layers such as the tachocline or other subsurface sections. Moreover, the oblateness of the Sun is directly linked to the quadrupole moment, a quantity which gives us information on the solar potential distortion. In this paper, the behavior of the oblateness ε, from the core to the surface, is carefully investigated, to understand how each layer of the Sun is affected by the differential rotation, and how each of these layers reacts to the perturbation of the potential. The shape of the profiles of ε, computed as a function of the radius and of the latitude, leads us to determine its theoretical value at the surface.

Several studies and observations have been undertaken since 1966 to evaluate the solar oblateness. The measurements began with the Princeton Solar Distortion Telescope, and yielded the first evaluation of the ellipticity of the Sun. Dicke and Goldenberg found a value for ε as large as $(4.51 \pm 0.34).10^{-5}$, a revisited value, deduced from the original data (Dicke and Goldenberg, 1967), taking into account all corrections for the seeing effects (Dicke and Goldenberg, 1974). In 1968, Goldreich and Schubert showed that the theoretical maximum solar oblateness, consistent with the stability of the Sun, is $3.5.10^{-4}$. They emphasized the fact that this value was consistent with the gradients of mean molecular weight, as calculated in standard solar models at that time. In 1975, Hill and Stebbins gave an intrinsic visual value of the difference between equatorial and polar diameters: $\Delta d = (18.4 \pm 12.5)$ milli arcsecond (mas) or $\varepsilon = (9.58 \pm 6.51).10^{-6}$. They extracted this value from observations influenced by an excess brightness, monitored at the same time to evaluate the necessary corrections. Then, in 1983, Kislik considered what effect the oblateness of the Sun might have on the astrometric (radar, optical) determinations of planetary orbits. He looked for the residuals of parameters determined from various kinds of observations, when the equations of planetary motion do not allow for the solar oblateness. In this study, he estimated that ε should be in the range $1.08.10^{-5} < \varepsilon < 2.69.10^{-5}$ (Kislik, 1983). This same year, Dicke, Kuhn and Libbrecht made new measurements of the Sun's shape at Mount Wilson, with an improved version

of the Princeton Solar Oblateness Telescope, which has been used in 1966. The measurements of the solar oblateness yielded a value $\Delta r = (19.2 \pm 1.4)$ mas or $\varepsilon = (2.00 \pm 0.14).10^{-5}$ (Dicke et al., 1985), the upper bound being only half of that observed in 1966: $\Delta r = 41.9 \pm 3.3$ mas. The data obtained in 1984 by Dicke et al. (1986) lead to significantly lesser values than those obtained in 1983: $\Delta r = (5.6 \pm 1.3)$ mas or $\varepsilon = (5.83 \pm 1.35).10^{-6}$. The 1985 data yielded a value $\Delta r = (14.6 \pm 2.2)$ mas or $\varepsilon = (1.52 \pm 0.23).10^{-5}$, which comes in between the 1984 and 1983 values of the solar oblateness (the 1984 value being the lowest). The authors concluded (Dicke et al., 1987) that the quantity Δr may vary with the 11.14 yr period of the solar cycle. In 1986, assuming that the Sun is in hydrostatic equilibrium, Bursa (1986) gave a new estimation of the Sun's oblateness range: $1.1.10^{-5} < \varepsilon < 2.7.10^{-5}$, where the upper limit requires a heavy core and the lower one corresponds to a nearly homogeneous body. In 1990, on the basis of radar observations, Afanas'eva et al. determined the quadrupole moment of the Sun by methods of celestial mechanics and deduced a range for the oblateness of the Sun from the theory of the figures of celestial bodies, assuming that the Sun rotates as a rigid body. They found: $10.8.10^{-6} < \varepsilon < 15.8.10^{-6}$. Motivated by the suggestion of Dicke, Kuhn and Libbrecht, that the magnitude of the oblateness might be a function of the solar cycle, Maier, Twigg and Sofia gave, in 1992, their preliminary results of the solar diameter from a balloon flight of the Solar Disk Sextant (SDS) experiment. They found $\varepsilon = (5.6 \pm 6.3).10^{-6}$ for the solar oblateness, but $\sim 30°$ offset from the polar-equator position. Additional studies, based upon flights in 1992 and 1994 (Lydon and Sofia, 1996), lead to a measured oblateness of respectively $(9.17 \pm 1.25).10^{-6}$ and $(8.77 \pm 0.99).10^{-6}$, indicating little or no variation. At the same time, from July 1993 to July 1994, Rösch et al. conducted observations at the Pic-du-Midi observatory by means of a scanning heliometer, which operates by fast photoelectric scans of opposite limbs of the Sun. Over this period, Rozelot & Rösch (1997) reported $\Delta r = (11.5 \pm 3.4)$ mas or $\varepsilon = (1.20 \pm 0.35).10^{-5}$, a value averaged from observations made in 1993 and 1994. New campaigns, conducted in 1995 and 1996, lead respectively to $\Delta r = (5.5 \pm 3.1)$ mas and $\Delta r = (8.9 \pm 2.1)$ mas (Rozelot, 1997). At last, Kuhn et al. (1998), found with the data obtained on board of the SOHO spacecraft, that the Sun's shape and temperature vary with the latitude in an inexpectedly complex way. The autors concluded also that the solar oblateness itself presents no strong evidence of varying with the solar cycle.

From the above reported data, two conclusions can be drawn, one concerning the observational values and the other one, the theoretical values. As far as the first one is concerned, a general agreement seems to exist on the fact that ε does not exceed $1.2.10^{-5}$, the averaged value being a bit below, around 6.10^{-6}. It is not yet clear if a solar cycle dependence is real or not; in such a case the amount of variation would be no more than 6.10^{-6}. All these values are of importance to constrain the solar models and it is not yet obvious if the global shape of the Sun follows a perfect ellipsoid or not. This point will be discussed later on (Sect. 4.4). As far as the theoretical values are

concerned, one could accept from the above quoted data that ε would lie around 9.10^{-6}. It is then of high interest to determine ε using one of the most recent solar models of mass and density combined with an up-to-date rotational model, which depends both on the latitude and on the distance to the rotation axis. This rotational model derives from helioseismological observations of p-mode rotational frequency splitting, deduced from measurements made on board the SOHO spacecraft. Observational data of high quality obtained from this satellite allowed Pijpers (1998) to determine an excess of the equatorial diameter on the polar diameter by some 0.017 arcsecond (Note, 1998).

In the following sections, we present the theoretical method of calculation and the models used to obtain the oblateness ε (Sect. 2). Next, we give the results and their interpretations (Sect. 3). Finally, we discuss the relation between the behavior of ε and the particular aspects of the solar interior (Sect. 4).

2. Theoretical approach

In this work, we consider the theory of a solar gravitation figure to include the effects of differential rotation. The oblateness can be defined as the difference between the equatorial and polar radii, usually expressed in milliarcsecond, or as a dimensionless coefficient defined by

$$\varepsilon = \frac{R_E - R_P}{R_E} \tag{1}$$

where R_E and R_P are the equatorial and the polar radius, respectively. This oblateness is linked to the quadrupole moment, that is to say to the potential describing the distribution of mass and velocity inside the Sun. This potential is deduced from the basic figure for steady rotation around a fixed axis (forming the zero-order approximation), with small corrections that can be successively added. Among several possible definitions of the solar surface, one of the best is to define it by a surface of constant gravitational potential, which permits one to treat the problem with a very high accuracy. This gravitational potential is usually developed into spherical harmonics, i.e. the Legendre polynomials P_{2n}. The even terms are only kept as the figure shows a symmetry created by the rotation around the minor axis. To this gravitational potential must be added the potential due to the rotation of the Sun, so that the total potential U_T is:

$$U_T = -\frac{GM_\odot}{R_E} \left[\frac{R_E}{r} - \sum_{n=1}^{\infty} J_{2n} \left(\frac{R_E}{r} \right)^{2n+1} P_{2n}(\sin\phi) \right] \tag{2}$$
$$-\frac{1}{2}\Omega^2 r^2 \cos^2\phi$$

where G is the gravitational constant, R_E the equatorial radius, $M_\odot$ the solar mass, r the solar radial vector (taken here as a variable), P_{2n} the Legendre polynomials, ϕ the latitude, Ω the rotation and J_{2n} the coefficients associated with the dynamical form of the Sun. According to the magnitude of the J_{2n} coefficients, the distortion from a pure sphere is more or less large. Due to the monotonic decreasing function of the distribution of mass in the solar case, the contribution of the first coefficient

is the most important and consequently signs the oblateness. To describe this oblateness, we express the ellipsoid shape in Cartesian coordinates:

$$\frac{x^2}{R_E^2} + \frac{y^2}{R_P^2} = 1 \tag{3}$$

Using the oblateness definition given by Eq. 1 and introducing the latitude ϕ, the following expression is obtained:

$$\frac{R_E}{r} = \cos^2\phi + (1 - \varepsilon)^{-2}\sin^2\phi \tag{4}$$

Developing Expression 4 up to the third order:

$$\frac{R_E}{r} = 1 + \varepsilon\sin^2\phi + \frac{\varepsilon^2}{2}(3\sin^2\phi - \sin^4\phi) + \bigcirc(\varepsilon^3) \tag{5}$$

Expression 5 is solved to obtain r, and using the binomial expansion, we find:

$$r = R_E\left[1 - \varepsilon\sin^2\phi + \frac{3}{2}\varepsilon^2(\sin^4\phi - \sin^2\phi) + \bigcirc(\varepsilon^3)\right] \tag{6}$$

Eqs. 2, 5 and 6 can be combined to express the total potential U_T limited to the second order as:

$$\begin{aligned} U_T = &-\frac{GM_\odot}{R_E}\Big[1 + a(\varepsilon,\phi) + J_2 b(\varepsilon,\phi) \\ &+ J_4 c(\varepsilon,\phi) + \frac{1}{2}\chi d(\varepsilon,\phi)\Big] \end{aligned} \tag{7}$$

where $a(\varepsilon,\phi)$, $b(\varepsilon,\phi)$, $c(\varepsilon,\phi)$ and $d(\varepsilon,\phi)$ are functions of the oblateness and the latitude, and $\chi = \frac{\Omega^2 R_E^2}{GM_\odot}$. At the equilibrium on the surface, the coefficients of J_2 and J_4 must vanish, so that, and after some algebra (see for instance Cole, 1978):

$$J_2 = \frac{2}{3}\varepsilon - \frac{\chi}{3} - \frac{\varepsilon^2}{3} + \frac{3}{7}\varepsilon\chi \tag{8}$$

$$J_4 = -\frac{4}{5}\varepsilon^2 + \frac{4}{7}\chi\varepsilon \tag{9}$$

Assuming that the Sun is symmetric around its axis of rotation and introducing spherical polar coordinates (r,θ,φ), the hydrostatic equation inside the Sun takes the well known form (see also Roxburgh, 1964, Paternó, 1996 and Pijpers, 1998):

$$\frac{\partial P}{\partial r} = -\rho\left(\frac{\partial\Phi}{\partial r}\right) + \frac{2}{3}\rho\Omega^2 r(1 - P_2(\cos\theta)) \tag{10}$$

$$\frac{\partial P}{\partial\theta} = -\rho\left(\frac{\partial\Phi}{\partial\theta}\right) - \frac{1}{3}\rho\Omega^2 r^2\frac{\partial P_2(\cos\theta)}{\partial\theta} \tag{11}$$

where P is the pressure, ρ the density, $P_2(\cos\theta)$ the second Legendre polynomial, θ the colatitude, and Φ the gravitational potential satisfying the Poisson equation:

$$\nabla^2\Phi = 4\pi G\rho \tag{12}$$

By cross-differentiation of Eqs. 10 and 11, P is eliminated; taking into account Eq. 12, the following dimensionless differential equation is obtained:

$$\frac{d^2 y}{dx^2} + \frac{2}{x}\frac{dy}{dx} - \frac{(6 + UV)}{x^2}y = \tag{13}$$

$$\frac{UV}{3}w^2 + \frac{2Uw}{3}\left(x\frac{dw}{dx} + \tan\theta\frac{dw}{d\theta}\right)$$

where the quantities $x = \frac{r}{R_\odot}$ and $y = \frac{\phi_2(r,\theta)}{\Omega_\odot^2 R_\odot^2}$ have been introduced dimensionless, as well as $U(x) = \frac{4\pi\rho R_\odot^3 x^3}{M_\odot M_x}$, $V(x) = \frac{d\ln\rho}{d\ln x}$ and $w(x,\theta) = \frac{\Omega(x,\theta)}{\Omega_\odot}$. The quantity $\Omega_\odot$ is the reference rotation rate, which is taken equal to the rotation rate of the radiative zone (for our purpose, this rotation rate is taken equal to 435 nHz). The second member of this differential equation contains the term of the rotation. Two approaches can be made. The first one consists in trying to give an analytical form of the solution y, and this have been made by Pijpers (1998). The oblateness is deduced from an inverse problem when the kernels of the integral relation are known. The other approach consists of solving Eq. 13 on successive shells of thickness $(dr\prime)$, taking into account at each step the boundary conditions. This method allows us to compute the succesive ellipticities of a stratificated Sun. The helioseismic constraints will play an important role in the adopted model of density and in the internal and differential rotation laws. This last method permits one to have access the local distortion of each small volume element in the Sun.

The differential Eq. 13 can be easily solved to obtain $\phi_2(r,\theta)$ if two boundary conditions are known. The first one is obvious, as the perturbation must vanish at the center. The second one (bearing in mind that Φ varies as $1/r^3$) is given by the continuity of Φ and $\frac{d\Phi}{dr}$ when crossing the surface of the Sun. These two conditions give:

$$\left\{\begin{array}{c}\phi_2 = 0 \text{ at } r = 0 \\ 3\phi_2 + r\frac{d\phi_2}{dr} = 0 \text{ at } r = R_\odot\end{array}\right\} \tag{14}$$

which can be rewritten in the dimensionless form:

$$\left\{\begin{array}{c}y = 0 \text{ at } x = 0 \\ 3y + x\frac{dy}{dx} = 0 \text{ at } x = 1\end{array}\right\} \tag{15}$$

Since the centrifugal force is a first order term, the density in the last term in Eq. 10 can be replaced by the zero-order spherically symmetric density. This term contains only zero and second Legendre coefficients. This leads us to expand the gravitational potential Φ in the form:

$$\Phi = \phi_0(r) + \phi_2(r,\theta)P_2(\cos\theta) \tag{16}$$

where ϕ_2 is a first order term. As outside the Sun, the gravitational potential satisfies the Laplace equation:

$$\Phi(r,\theta) = -\frac{GM_\odot}{r}\left[1 - J_2\left(\frac{R_\odot}{r}\right)^2 P_2(\cos\theta)\right] \tag{17}$$

The identification of the same order terms in Eqs. 16 and 17 leads, whatever θ is, to:

$$\phi_2(r,\theta) = J_2\left(\frac{R_\odot}{r}\right)^2\frac{GM_\odot}{r} \tag{18}$$

hence,

$$J_2 = \frac{\phi_2(r,\theta)}{R_\odot^2\Omega_\odot^2}\frac{\Omega_\odot^2 r^3}{GM_\odot} \tag{19}$$

or

$$J_2 = y(r, \theta) \frac{\Omega_\odot^2 r^3}{GM_\odot} \tag{20}$$

The heterogeneous composition of the internal layers of the Sun are here represented as a series of successive thin shells, the composition of each shell being homogeneous. The oblateness ε' can be computed for each of these shells assuming that the matter which is outside a shell of a given radius $r'_\odot$, is in the outer space and satisfies Eqs. 14.

From Eq. 8 limited to the first order, the oblateness at the distance $r\prime$ is expressed for a shell as:

$$\varepsilon'(r'_\odot, \theta) = \frac{3}{2} J'_2(r'_\odot, \theta) + \frac{1}{2} \frac{\Omega'^2_\odot r'^3_\odot}{GM_\odot} \tag{21}$$

Hence, according to the potential,

$$\varepsilon'(r'_\odot, \theta) = \frac{\Omega'^2_\odot r'^3_\odot}{GM_\odot} \left(\frac{3}{2} y(r'_\odot, \theta) + \frac{1}{2} \right) \tag{22}$$

where $r'_\odot$, $M'_\odot$ and $\Omega'_\odot$ are respectively the radius, the mass and the rotation rate of a shell of thickness dr'. Note, that when integrating $\varepsilon'(r'_\odot, \theta)$ over the whole radius of the Sun, this would lead to a global figure of the Sun which will change with the latitude. This is one of the main features of this paper: the helioid (just as the geoid, but obviously at a very lower degree) is not perfectly ellipsoidal.

A mass and density model for the Sun is required to solve the differential Eq. 13. We have chosen one of the five solar models of Richard et al. (1996) - Model 3 - including the helioseismological constraints. This model is computed with element segregation and with Grevesse values as initial abundances, iterated so that the final abundances are also those given by Grevesse (1991). Moreover, the element segregation, introduced in Model 3, has shown that it fits very well the seismic data.

As the solar rotation depends both on the radial distance and on the colatitude, we need to define a law to express $\Omega(r, \theta)$. Among several laws available, we have chosen that proposed by (Kosovichev, 1996b), which is based on the observed p-mode rotational frequency splittings. The law is represented in terms of associated Legendre functions of order 1, $P_k^1(\theta)$:

$$\frac{\Omega(r, \theta)}{2\pi} = \sum_{k=0,1,2} \alpha_k A_{2k+1}(r) \frac{P_{2k+1}^1(\theta)}{\sin \theta} \tag{23}$$

where

$$\alpha_k = (-1)^{(k+1)} \frac{k! 2k}{(2k+1)!!} \tag{24}$$

and $A_k(r)$ is a radial function developed in a parametric form. From the analysis of the Big Bear Solar Observatory data, Kosovichev formulates a simple model of solar rotation based on the first three terms of expansion 23 ($x = \frac{r}{R_\odot}$):

$$\frac{\Omega(r, \theta)}{2\pi} = A_1(x) + A_3(x) \left[1 - 5 \cos^2 \theta\right] \tag{25}$$
$$+ A_5(x) \left[1 - 14 \cos^2 \theta + 21 \cos^4 \theta\right]$$

From a numerical point of view, with the value of A_k given in nHz, Eq. 25 is expressed by:

$$A_1(x) = \left\{ \begin{array}{cc} 435 & x \leq 0.71 \\ 435 + 51.85(x - 0.71) & 0.71 \leq x \leq 0.983 \\ 435 - 882.53(x - 1) & 0.983 \leq x \leq 1 \end{array} \right\} \tag{26}$$

$$A_3(x) = 22\phi(x) \tag{27}$$

$$A_5(x) = -3.5\phi(x) \tag{28}$$

where

$$\phi(x) = 0.5 \left(1 + \mathrm{erf} \left[2 \frac{(x - 0.69)}{0.1} \right] \right) \tag{29}$$

This model is particularly valued owing to its analytical form describing fairly well the differential rotation of the convective zone and the rigid rotation of the radiative zone, and not depending on the density ρ. For lack of data concerning the g-modes, it is not yet possible to know if the rotation in the core is faster or slower than the rotation of the radiative zone. Thus, we adopt the same rotation rate for the core and for the radiation zone: ~ 435 nHz.

3. Determination of the oblateness

Differential Eq. 13 was solved to obtain the function of the potential $y(r, \theta)$ and to deduce through Eq. 22 the behavior of ε, shell by shell, for different latitudes: 0, 15, 30, 45, 60, 75 and 90 degrees. The numerical integration step is determined by the model. The number of steps has been taken as 220; to test the robustness of the solution, this sample has been extended up to 2100 steps and no significant difference has been found. For the numerical applications, the adopted values for the solar parameters are those given by Allen (1976): $R_\odot = 6.95997.10^8 m$ and $M_\odot = 1.9892.10^{30} kg$.

3.1. Study of the successive layers considered as thin shells

In this study, we consider simultaneously two types of rotation for the Sun: a global rigid rotation and a differential rotation computed with the above mentioned rotation law. The corresponding curves for a Sun splitted in successive shells, are shown in Fig. 1.

The profiles, which are computed for the rigid rotation $w = 1$ and for the differential rotation $\Omega(r, \theta)$, globally evolve identically up to $0.65 R_\odot$, then diverge up to the surface. Looking in more detail, the curve corresponding to $w = 1$ is shifted from the others as early as $0.3 R_\odot$. The curves present a first variation around $0.65 R_\odot$ and diverge. The curves, corresponding to $0°$, $15°$, $30°$, $w = 1$, $45°$ and $60°$ (in decreasing order of the latitudes) increase and present a second very slight variation near $0.71 R_\odot$. The curves corresponding to $75°$ and $90°$ decrease from $0.65 R_\odot$ up to $\sim 0.71 R_\odot$, then increase until a variation of the gradient around $0.78 R_\odot$, and those corresponding to $75°$ and $90°$ decrease up to $0.78 R_\odot$, then increase. From $0.78 R_\odot$,
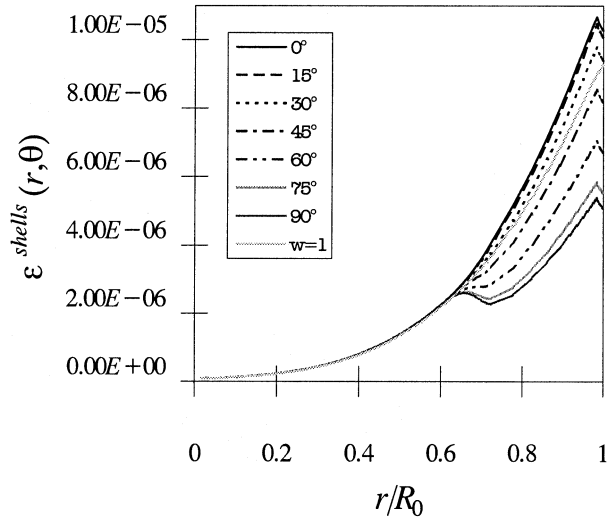
Fig. 1. Profile of the oblateness of the Sun splitted in successive shells and numerically computed both for the rigid rotation case $w(x, \theta) = \frac{\Omega(x,\theta)}{\Omega_R} = 1$ and the differential rotation case for latitudes 0, 15, 30, 45, 60, 75 and 90 degrees. Around $0.7R_\odot$, the passage of the transition zone is clearly visible.
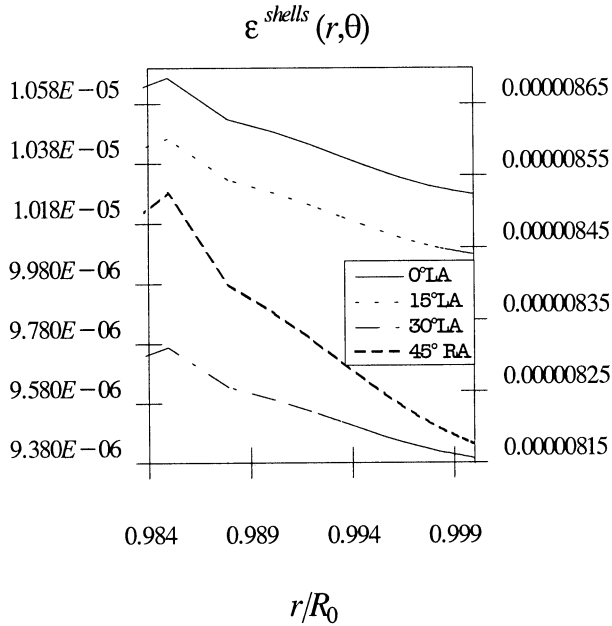

Fig. 2. Zoom of the right side of the previous global profiles (Fig. 1.) for the differential rotation case at 0, 15, 30 (Left Axis) and 45 degrees (Right Axis) to show two of the main changes of curvature located around $0.989R_\odot$ and $0.994R_\odot$.

each curve increases and reaches a maximum around $0.985R_\odot$ (Fig. 2.). In their decreasing, they all present two changes of curvature, located around $0.989R_\odot$ and $0.994R_\odot$. Only the curve corresponding to w=1 is globally increasing (Fig. 1.), but also presents two changes of curvature located around $0.984R_\odot$ and $0.993R_\odot$.

Above $0.999R_\odot$, a change of curvature is visible with a minimum near $0.99991R_\odot$ at latitudes 0, 15, 30, 45, and 60
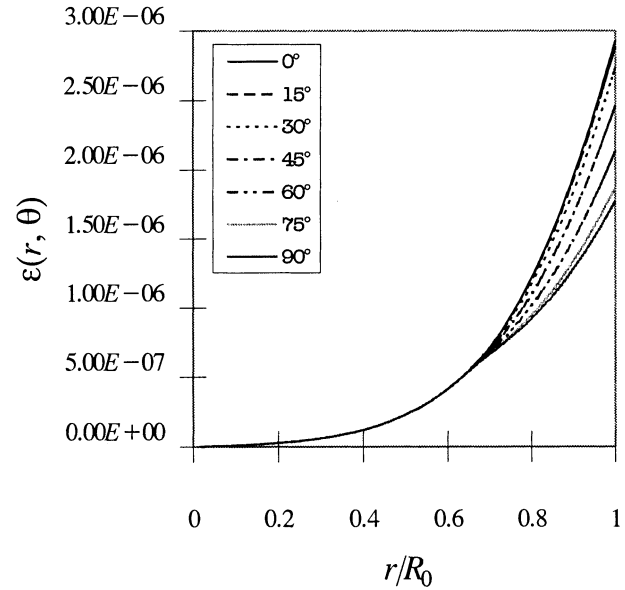

Fig. 3. Profiles of the oblateness of the Sun integrated on successive shells and depending upon the latitudes.

degrees. For latitudes 75° and 90°, the curves decrease without any clearly visible variation. Nevertheless, these ones are not completely linear around $0.99991R_\odot$, where a minimum appears. In the same range, the curve corresponding to $w = 1$ increases presenting a very slight minimum near $0.99991R_\odot$. The oblateness being directly linked to the solar potential, it will be modified in a region where this potential is affected by flows or events.

These detected variations can be linked to the borderline of the shear layer which governs the transitions between the different zones within the Sun. In the following discussion, we present a synthesis of actual results and we propose a scenario for the structure of the solar layers.

3.2. The radial integration case

This computed oblateness behavior is consistent with the differential rotation law expressing that the higher the rotation rate of a shell, the higher the amount of ε. The integration over each shell yields the behavior of ε for a body of radius $r_\odot$ that can be expressed at each given latitude (Fig. 3.).

$$\varepsilon(x, \theta') = \sum_{x'} \varepsilon(x', \theta') \Delta x' \qquad (30)$$

where x' is associated to the radius of the shells.

These integrated curves diverge near $0.68R_\odot$ and present for some of them a slight variation located approximately at $0.72R_\odot$. Then, they increase to reach a stable value near the surface.

To compare this theoretical model with available observations, we also present the profiles (Fig. 4.) which illustrate the latitudinal variation of the solar semi diameter observed by means of the solar astrolabe at CERGA in France (Laclare et al., 1996) and in Santiago, Chili (Noël, 1999). These
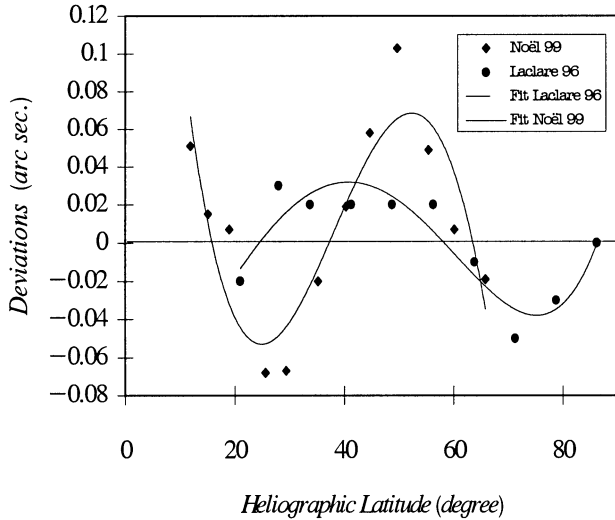
Fig. 4. Deviations from the mean solar semi diameter, deduced from the observations obtained by means of a solar astrolabe by F. Laclare (1996) at CERGA in France and by E. Noël (1999) in Santiago, Chili.

data are compared with our results. The observational results of F. Laclare show that the largest ellipticity is obtained for $0°$ (by extrapolation), $30°$, $45°$ and $90°$, and the more oblate regions are located at $60°$ and $75°$. The observational results of E. Noël show that the largest ellipticity is obtained for $0°$ (by extrapolation), $15°$, $45°$ and $60°$, and the more oblate regions are located at $30°$, $75°$ and $90°$. The latitudinal order of our curves presents the order in which the solar regions are the most elliptic (large curvature) towards the most oblate regions. The largest ellipticity is obtained for $0°$, then $15°$ and $30°$. The Sun is less elliptic at $75°$ and $90°$, which indicates a possible bump around the royal zones centered on $60°$.

3.3. The latitudinal integration case

The sum of the radial integrated oblatenesses over all heliographic latitudes yields the total behavior of ε (Fig. 5.).

$$\varepsilon(x, \theta) = \sum_{\theta'} \varepsilon(x, \theta') \Delta \theta' \tag{31}$$

The model used stops at $0.99998 R_\odot$, but we can extrapolate the curve of the integrated profile, without a too large error on the final result. So, the oblateness of the Sun can be determined as

$$\varepsilon = 8.77.10^{-6} \tag{32}$$

Comparing the profile of ε for the differential rotation case with the profile of ε in the rigid rotation case, where we find $\varepsilon_0 \simeq 2.59.10^{-6}$, we see that the oblateness of the Sun is increased by the differential rotation of a quantity equal to $6.18.10^{-6}$ (Fig. 6.).

4. Discussion

In our study, the determination of the integrated value of ε over r and θ leads to $\varepsilon = 8.77.10^{-6}$ at the surface of the Sun (that is to
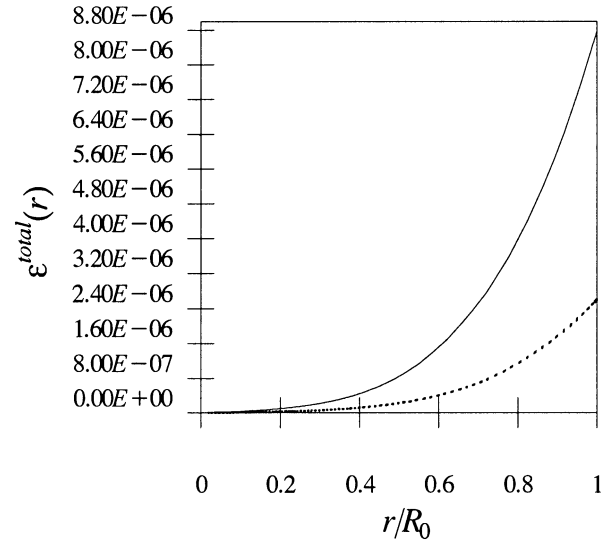

Fig. 5. Profiles of the integrated oblatenesses of the Sun. The plain curve is computed, taken into account the differential rotation by means of helioseismic data. The dashed curve is obtained in the case of rigid rotation $w = 1$.
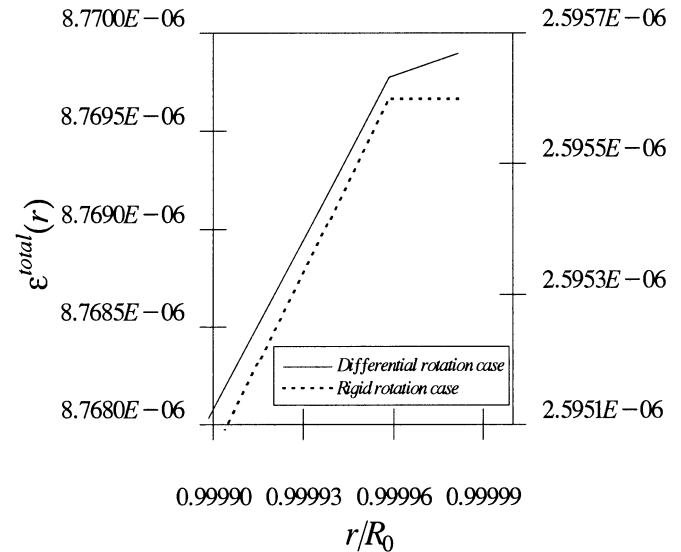

Fig. 6. Zoom of the right side of the previous profiles (Fig. 5.) in the differential rotation case and in the rigid rotation case, to determine the value of oblateness at the surface in these two cases. The plain curve permits us to determine $8.77.10^{-6}$ for the oblateness in the differential rotation case and $2.59.10^{-6}$ in the rigid rotation case. Note the break which appears at $0.99996 R_\odot$.

say J_2 equal to $1.60.10^{-7}$ (Godier and Rozelot, 1999)). These values are sightly weaker in comparaison to the values quoted in the introduction of this paper and also in comparaison to the values obtained by Pijpers (1998) deduced from the ponderate GONG and MDI data, that is to say $(2.18 \pm 0.06).10^{-7}$. The main reason comes from the assumptions made in the computations, which are slightly reductive. In a first approach, and to improve these assumptions, one could change the boundary conditions. In a second study, one should take into account the varia-

tion of temperature at the surface of the Sun (Kuhn et al., 1998), if any. This variation would question the assumption of the hydrostatic equilibrium and of the equipotential surfaces. On the other hand, the chosen assumptions are sufficient, for the time being, to study and interpret the profiles of oblateness. Indeed at least two observations have been made to attempt to measure the successive moments in order to be free from the atmospheric turbulences. The first one has been made by Lydon and Sofia (1996) which found $1.8.10^{-7}$ for J_2 and $9.8.10^{-7}$ for J_4. The second one has been performed by Kuhn et al. (1998) which report along a Legendre expansion of the measurements made on board the SOHO spacecraft on March 1997, a quadrupolar distortion (l=2; the oblateness) of 5.18 ± 0.44 mas and a hexadecapole shape term (l=4) of 1.37 ± 0.54 mas. The l=4 value are of very high amount and in complete contradiction with Eq. 9. To be perfectly self consistent with the formalism, it must be noted that $J_2(\theta)$ which is in fact a differential form of J_2, must not be confused with the l=4 coefficient. A paper under preparation will bring more detailed comments on that multipole moments applied to the Solar case.

4.1. The properties of the tachocline

The profile of ε is one of the direct information through which the latitudinal variation of the solar quantities can be reached, such as the position of the center or the width of the transition layers. The first perturbed layer, located between $0.60R_\odot$ and $0.75R_\odot$, where the rotation rate changes from differential rotation in the convection zone to an almost latitudinally independent rotation rate in the radiative interior, is called the tachocline (Spiegel and Zahn, 1992). The helioseismic data show that this region of rapid change has its center located only slightly below the convective zone (Charbonneau et al., 1999) at $(0.693 \pm 0.017)R_\odot$, and that the thickness of this layer is $(0.039 \pm 0.017)R_\odot$. Current studies of this layer show that the tachocline is a shear layer and could accomodate the dynamo-effect and a magnetic field. In particular, the helioseismic data show that the endpoint of the adiabatically stratified part of the convection zone is located at $(0.713 \pm 0.003)R_\odot$ (Kosovichev, 1996a) and (Christensen-Dalsgaard et al., 1991). This would mean, that the tachocline ends where the convection zone begins. Nevertheless, if the tachocline becomes slightly thicker and shifts at higher latitudes, a part of the tachocline might be extended into the convection zone, at least at these latitudes (Basu and Antia, 1998) and (Antia et al., 1998); in this case, it is possible that the position of the base of the convection zone might also depend on the latitude. At $r = 0.713R_\odot$ (determined at the equator), the value of the oblateness varies with the latitude. So, according to the chosen latitude, the value of the position of the base of the convection zone can be larger or smaller than its position at the equator. Therefore, if the position of the base of the convection zone changes with the latitude, the position of the top also changes, not necessarily in phase with the base. This is clearly visible in Figs. 1 and 3, which show that when r is increasing, the departure between each profile is not constant. Thus, the properties of the tachocline, described

by the position of its center and its width, vary with the latitude. As the Sun is a bit more elliptic at the equator, each layer is thinner at the poles than at other latitudes: the tachocline would be certainly thinner near the poles than near the equator.

Charbonneau et al. (1999) suggest that the tachocline is *prolate* and may have a central radius larger at $60°$ than at the equator. This suggestion is directly deduced from the most recent helioseismic study of the differential rotation, and may not be contradictory to our result. This would simply mean that if a bump does exist around $60°$ of latitude, at the surface, and as previously seen, this geometry with a bump, is preserved inside the Sun.

4.2. The tachocline and the overshoot layer

Canuto (1998) suggests that the tachocline can originate in the part of the overshooting region, where the convective flux is still positive. Another scenario assumes that the solar dynamo has a measurable effect on the stratification of the overshoot layer where the magnetic field can be stored (Monteiro et al., 1998), if the convective flux inside this layer is negative. These two arguments would mean that the overshooting layer might be divided in two regions. The first one would be located at the base of the convection zone, where the convective flux is negative, that is, where the magnetic field is stored. The second region, where the convective flux would become positive, would correspond to a part of the tachocline. According to the values of the position of the center of the tachocline and the position of the base of the convection zone, the top of the tachocline is located at around $0.712R_\odot$ while the base of the convection zone is located at around $0.713R_\odot$. The difference in thickness, which accounts for approximately 700 km only, may be associated to the first overshoot layer, with a weak thickness, if this layer begins at the base of the convection zone. If this layer begins within the convection zone, this first part of the overshoot layer should be more extended. A priori, our model of oblateness, for a Sun splitted in shells, shows a variation in the curves near $0.71R_\odot$, more or less visible according to the latitude, and even more marked at the latitudes of $60°$, $75°$ and $90°$, which is typically associated to the borderline of the convection zone. Then, we observe on these same curves a weaker gradient up to $\sim 0.78R_\odot$ for latitudes $60°$, $75°$ and $90°$. This means that the oblateness does not vary along the radius for these considered latitudes until a certain depth, that defines a new region. As the length of the plateau is not the same according to the considered latitude, the thickness of this new region also varies with the latitude. This shows that this region could be associated with the extend of the first overshoot layer, whose thickness would be around $0.07R_\odot$: in this case, our model shows, if we can trust the helioseismic data, that the extension of this region would be larger, accounting for approximately 50000 km. In our opinion, this layer, which would accomodate the magnetic field, would be a transfer layer of the field. The dynamo-effect, located in the tachocline (not in the convection zone, to eliminate a radial propagation), would transform the poloidal field into a toroidal field, both stored in the transfer layer. Then, this toroidal field

would climb throughout the convection zone, up to the surface to produce the sunspots. Boruta (1996) estimated the limit strength of the magnetic field in a transition layer around 0.5G, but this value depends on the thickness of this layer. Recently, Tobias et al.(1998) proposed a scenario where the required transport of magnetic field, from the convection zone to the overshoot region, can be achieved on a convective timescale by a pumping mechanism in turbulent penetrative compressible convection. This scenario may explain the passage of the magnetic field from the transfer layer to the tachocline to sustain the dynamo-effect, but we do not have yet a scenario to explain the increase of the transformed magnetic field.

4.3. The structure of the subsurface

Apart from the tachocline, another shear layer near the solar surface has been put into evidence at about $0.95R_\odot$, where the rotation rate increases with depth (Antia et al., 1998). This shear layer has already appeared in our study of the quadrupole moment of the Sun (Godier and Rozelot, 1999). It is certainly directly linked to the passage from the convective zone to a new thin radiative layer (Richard et al., 1996) and (Morel et al., 1997), the top of which being the surface of the Sun. This layer is associated to several events which appear just below the surface, such as the meridional and zonal flows, or the seismic events and the jets. The meridional flows, large-scale mass motions from the equator to the poles, are located between $0.979R_\odot$ and $0.999R_\odot$ (Hernandez et al., 1999) and the velocities are predominantly poleward. The zonal flow bands have been detected with a velocity variation of 5 m.s^{-1} at a depth located between $0.987R_\odot$ and $0.997R_\odot$ beneath the surface from helioseismic MDI data (Kosovichev, 1997). These zonal bands, characterised by faster and slower rotation, and consistent with surface observations of the torsional oscillations, migrate towards the equator. The seismic events (or sunquakes) have been identified in the photosphere and seem generated by the collapse of the intergranular lane (Goode et al., 1998). The total duration of the expansive phase of the events is of about 5 minutes. These events are confirmed by Nigam and Kosovichev (1999) who found that the solar acoustic modes are excited in a thin superadiabatic layer of turbulent convection of about 75 ± 50 km (i.e. between $0.99982R_\odot$ and $0.99996R_\odot$) below the Sun surface. If we carefully examine the curves of our model in the region defined in the range $[0.979R_\odot; 0.999R_\odot]$, where the meridional and zonal flows are found, it is difficult to associate observed variations with a given flow. In any case, the maximum observed around $0.985R_\odot$ (Fig. 1. and 2.) can not be considered, because it depends on the Kosovichev rotation law which presents the same maximum at the same value of the radius. Apart from these maxima, we notice a first change of curvature around $0.989R_\odot$ for each latitude, and a second one around $0.994R_\odot$, at each latitude (less marked at 75 and 90 degrees). These two changes can be associated with the zonal and meridional flows. They both verify the definition range of these flows and one of them might be the signature of the zonal flows. These variations exist at each latitude and confirm the

faster and slower rotation of the bands. The other one might be the signature of the meridional flows, which circulate from the equator to the poles. These variations mean that the set of shells belonging to this range of values presents a larger oblateness than the previous shells and than the following ones. Around $0.9995R_\odot$, our curves present another change of curvature at latitudes 0, 15, 30, 45, and 60 degrees, which might be associated with a borderline of the layer. Indeed, from the surface up to this depth, the acoustic cutoff frequency is much larger (until 5000μHz) than in the solar interior ($< 600 \mu$Hz). The acoustic cutoff frequency is linked to the gradient of density which rapidly increases above $0.9995R_\odot$ (Corbard, 1998a). Here, we can remark that the curve, corresponding to a rigid rotation of the Sun ($w = 1$, plotted in Fig. 1.), presents the same variations around $0.984R_\odot$, $0.993R_\odot$ and $0.9995R_\odot$. This indicates that these variations are not brought by the rotation model but present a physical reality. Above $0.9995R_\odot$, we observe new variations for certain latitudes. At $0°$, $15°$ and $30°$, we have two changes of curvature and an increasing ended curve. At $45°$ and $60°$, we notice two changes of curvature and a decreasing ended curve. At $75°$ and $90°$, the curves do not clearly present variations, but we observe a slight shift to the linearity of the curves around $0.99991R_\odot$. The changes of curvature are located around $0.99989R_\odot$ and $0.99993R_\odot$. These values belong to the range $[0.99982R_\odot; 0.99996R_\odot]$ where the seismic events seem to take place. But, these seismic events would occur at precise latitudes, since we do not observe the same variation at every latitude. Our model does not present events near the poles. Concerning the jets, our model gives no variations around $0.95R_\odot$.

The comparison between the solar events and our model of oblateness, is very important to improve the understanding of the stucture of the subsurface. The shear layer beneath the surface is not without calling on the shear layer located around $0.7R_\odot$ and described in (Sect. 4.2). In these two cases, this transition represents the passage between a convection zone and a radiation zone, and thus we can assume that similar physical characteristics might be found again. The helioseismic data permit us to deduce an increasing of the rotation below the surface (with a maximum around $0.95R_\odot$) up to ~ 470 nHz (Corbard, 1998b). This value corresponds to the rotation of the small magnetic structures observed at the surface (Komm et al., 1993). This suggests that these structures might be stored around $0.95R_\odot$ (Corbard et al., 1997).

This set of considerations strongly suggests that, just below the surface, may exist a double layer which could be constituted in the same way as that of the transition region located at $0.7R_\odot$. The first layer would be a shear layer like the tachocline, located between $0.99950R_\odot$ (which seems to correspond to a borderline) and $0.99996R_\odot$, which would be the top of the convection zone, given by the observation of our integrated profile (Fig. 6.). The second layer would be an overshoot layer, extended from $0.95R_\odot$ up to $0.9995R_\odot$. In this layer, the magnetic field at small-scale would be stored and the zonal and meridional flows would circulate. This scenario of a double layer beneath the surface is also proposed by Basu et al. (1999) who gave a depth of $4 \text{ Mm} (\sim 0.994R_\odot)$ for the outer part. Thus, the seismic events

would happen at the base of the shear layer. In this approach, the shear layer would have a thickness of $0.00046R_\odot$ and the overshoot layer of $0.0495R_\odot$.

4.4. The variation of the solar radius with latitude

The profiles of the oblateness ε allow us to estimate the shape of the Sun with respect to the latitude. Our results show that the radius decreases slightly from the equator (latitude at which the radius is the largest), then at $15°$, $30°$, $45°$, $60°$, $75°$ up to $90°$ (latitude at which the radius is the smallest). At latitudes $0°$, $15°$, and $30°$, the radius is slightly larger than the mean radius. It is more difficult to give an estimation of the radius around $45°$, but the values found are sufficient to evaluate the shape of the Sun, which seems to present through our model, a lenghtening at the equator and a bump around $60°$. This estimation is globally in agreement with the observations of the semi diameter (Fig. 4.) made both by F. Laclare (1996) at CERGA in France and E. Noël (1999) in Santiago, Chili, by means of a solar astrolabe. The consistency of our model with the variability found through observations of the semi diameter shows that the data obtained from ground-based experiments seem to have a physical reality. Nevertheless, it seems that the observed difference between the two extreme values, is very large: 80 mas in the data given by F. Laclare and 170 mas in the data given by E. Noël. The oblateness deduced from Laclare's data would be larger than 10.10^{-5}, whereas we find an oblateness of $8.77.10^{-6}$.

5. Conclusion

In this analysis, we have determined the profiles of the solar oblateness ε, as a function of radius and latitudes, from the core to the surface, and we have given its theoretical integrated value at the surface. The method used has consisted in the computation of the differential equation governing the fluids in hydrostatic equilibrium which depends on the latitude. The main quantities, taking part in this computation, are the mass and the density, which respect the helioseismic constraints, and the rotation given by a parametric model derived from helioseismic data.

The main results obtained are the following:

- The theoretical value, at the surface, of the solar oblateness is $\varepsilon = 8.77.10^{-6}$.

- From the model used, ε can be drawn as a function of the solar radius (assuming the Sun set up of successive homogeneous thin shells) and of the latitude. The variation of ε with the latitude shows that the properties of the tachocline, such as the width and the position of the center, vary with the latitude.

- The gradient which occurs in the profiles of $\varepsilon(r)$, plotted for successive shells, from $0.71R_\odot$ up to $0.78R_\odot$, sets borderlines of a new region located between the tachocline and the convection zone. This overshoot layer may have a joint zone with the tachocline, where the convective flux would be positive. The properties of this layer should also vary with the latitude.

- Beneath the surface, our model of oblateness gives changes of curvature in the profiles, which can be connected to solar events. The two first are located at $0.989R_\odot$ and at $0.994R_\odot$. They are certainly linked to two types of flows: the zonal flows, represented by bands, and the meridional flows which circulate from the equator to the poles. The third change is located at $0.9995R_\odot$ and can be associated with the layer's borderline. Then, the fourth and fifth changes, which occur at $0.99989R_\odot$ and at $0.99993R_\odot$, can be the signature of the region where the seismic events take place.

- A transition zone, characterised by the passage from a convective zone to a radiative one, exists inside the tachocline and within the subsurface. We assume that the structure of these two different transition layers may be similar. On this basis, we showed that the transition zone within the subsurface is composed of two layers, the first one has an extension in the range $[0.9995R_\odot, 0.99996R_\odot]$; the second one, where the magnetic field would be stored, extends in the range $[0.95R_\odot, 0.9995R_\odot]$.

- Finally, we were able to deduce from this study a global shape of the Sun, and we confirm that the solar diameter presents a dependence on the latitude.

The full study of a differential rotating body, such as the Sun, leads to the conclusion that the exact shape critically depends both on the rotation law from the subsurface to the tachocline and on the properties of its internal structure: shear, magnetic field, flux of matter, seismic events, etc... A motivating objective would be to monitor the solar parameters, like the oblateness, from space.

References

Afanas'eva, T. I. and Kislik, M. D.: 1990, Sov. Astronomy 34 (6)

Allen, C. W.: 1976, Astrophysical Quantities, The Athlone press, Third Edition

Antia, H. M., Basu, S., and Chitre, S. M.: 1998, MNRAS 298, 543

Basu, S. and Antia, H. M.: 1998, in S. Korzennick and A. Wilson (eds.), Structure and Dynamics of the Interior of the Sun and Sun-Like Stars, pp 711–715, ESA, Boston USA, SOHO6 / GONG 98 Workshop (SP-418)

Basu, S., Antia, H. M., and Tripathy, S. C.: 1999, ApJ 512, 458

Boruta, N.: 1996, ApJ 458, 832

Bursa, M.: 1986, Bull. Astronom. Inst. 37, 312

Canuto, V. M.: 1998, ApJ 497, 51

Charbonneau, P., Christensen-Dalsgaard, J., Henning, R., et al.: 1999, ApJ, To be published

Christensen-Dalsgaard, J., Gough, D. O., and Thompson, M. J.: 1991, ApJ 378, 413

Cole, G. H. A.: 1978, The Structure of the Planets, Chapt. III. External figure of a planet and its gravity and IV. Internal conditions and hydrostatic equilibrium, pp 31–62, The Wykeham Science Series, Wykeham publications

Corbard, T.: 1998a, Physics sciences, Universite de nice - Sophia Antipolis, Observatoire de la Côte d'Azur, Thesis

Corbard, T.: 1998b, La Rotation Interne Du Soleil Déduite de L'héliosismologie, Cours pour l'école d'aussois, Cours d'Aussois

Corbard, T., Berthomieu, G., Morel, P., et al.: 1997, Astron. Astrophys. 324, 298

Dicke, R. H. and Goldenberg, H. M.: 1967, Phys. Rev. Lett. 18(9), 313

Dicke, R. H. and Goldenberg, H. M.: 1974, ApJ Suppl. 27, 131

Dicke, R. H., Kuhn, J. R., and Libbrecht, K. G.: 1985, Nature 316, 687

Dicke, R. H., Kuhn, J. R., and Libbrecht, K. G.: 1986, ApJ 311, 1025

Dicke, R. H., Kuhn, J. R., and Libbrecht, K. G.: 1987, ApJ 318, 451

Godier, S. and Rozelot, J. P.: 1999, Astron. and Astrophys. 350, 310

Goldreich, P. and Schubert, G.: 1968, ApJ 154, 1005

Goode, P. R., Strous, L. H., Rimmele, T. R., et al.: 1998, ApJ 495, 27

Grevesse, N. and Anders, E.: 1991, in Solar Interior and Atmosphere, pp 1227–1234, University of Arizona Press, Tucson, AZ, Appendix A

Hernandez, I. G., Patron, J., Bogart, R. S., et al.: 1999, ApJ 510, L153

Hill, H. A. and Stebbins, R. T.: 1975, ApJ 200, 471

Kislik, M. D.: 1983, Sov. Astro. Lett. 9(5), 296

Komm, R. W., Howard, R. F., and Harvey, J. W.: 1993, Sol. Phys. 143, 19

Kosovichev, A. G.: 1996a, ApJ 469, 61

Kosovichev, A. G.: 1996b, in J. Provost and F. X. Schmider (eds.), Sounding Solar And Stellar Interiors, pp 97–98, IAU, Kluwer Academic Publishers, Nice France, Symposium N185, Poster Volume

Kosovichev, A. G.: 1997, ApJ 482, 207

Kuhn, J. R., Bush, R. I., Scheick, X., et al.: 1998, Nature 392, 155

Laclare, F., Delmas, C., Coin, J. P., et al.: 1996, Solar Physics 166, 211

Lydon, T. J. and Sofia, S.: 1996, Physical Review Letters 76(2), 177

Maier, E., Twigg, L., and Sofia, S.: 1992, ApJ 389, 447

Monteiro, M. J. P. F. G., Christensen-Dalsgaard, J., and Thompson, M. J.: 1998, in S. Korzennik and A. Wilson (eds.), Structure and Dynamics of the Interior of the Sun and Sun-Like Stars, pp 495–498, ESA, Boston USA, SOHO 6 / GONG Workshop, SP-418

Morel, P., Provost, J., and Berthomieu, G.: 1997, Astron. Astrophys. 327, 349

Nigam, R. and Kosovichev, A. G.: 1999, ApJ 514, L53

Noël, E.: 1999, Astron. Astrophys. 343, 1001

Note, N.: 1998, Sky and Telescope "Sounding out our swollen Sun" from F. Pijpers, 22

Paterno, L., Sofia, S., and Di-Mauro, M. P.: 1996, Astron. Astrophys. 314, 940

Pijpers, F. P.: 1998, MNRAS 297, 76

Richard, O., Vauclair, S., Charbonnel, C., et al.: 1996, Astron. Astrophys. 312, 1000

Roxburgh, I. W.: 1964, Icarus 3, 92

Rozelot, J. P.: 1997, in B. Donahue and J. Bookbinder (eds.), The Tenth Cambridge Workshop on Cool Stars, Stellar Systems and the Sun, p. 685

Rozelot, J. P. and Rösch, J.: 1997, Solar Physics 172, 11

Spiegel, E. A. and Zahn, J. P.: 1992, Astron. Astrophys. 265, 106

Tobias, S. M., Brummel, N. H., Clune, T. L., et al.: 1998, ApJ 502, L177